No 498

MAY 2022

CefES

Center for European Studies

PAPER SERIES

Is Climate Change Time Reversible?

Francesco Giancaterini, Alain Hecq, Claudio Morana

DIPARTIMENTO DI ECONOMIA, METODI QUANTITATIVI E STRATEGIA DI IMPRESA

UNIVERSITA' DEGLI STUDI DI MILANO BICOCCA

Is climate change time reversible?

Francesco Giancaterini [1a], Alain Hecq[a], Claudio Morana[b]

[a]*Maastricht University*
[b]*University of Milano-Bicocca*
Center for European Studies -Milan
RCEA-Europe ETS
CeRP - Collegio Carlo Alberto

Abstract

This paper, exploiting the properties of mixed causal and noncausal models, proposes strategies to detect time reversibility in stationary stochastic processes. We show that they can also be used for nonstationary processes when the trend component is computed using the Hodrick-Prescott filter characterized by a time-reversible closed-form solution. We then establish a linkage between the concept of environmental tipping point and the statistical property of time irreversibility and investigate nine climate indicators. While we detect time irreversibility in GHG emissions, global temperatures and fundamental natural oscillations do not show this feature. Under a constructive view, our findings then give hope that correction policies might still help avoid the worst consequences of climate change.

Keywords: mixed causal and noncausal models, time reversibility, global warming, generalized Student's t-distribution, Hodrick-Prescott filter.
JEL: C22

1. Introduction

According to the most recent International Panel on Climate Change report, humanity is unlikely to prevent global warming by 1.5° above pre-industrial levels. Still, aggressive curbing of greenhouse-gas emissions and carbon extraction from the atmosphere could limit its rise and even bring it back down (IPCC (2022)). But this window is rapidly closing, and, above the 1.5° limits, the chances of tipping points, extreme weather, and ecosystem collapse will become even more sizeable.

An environmental tipping point is when small changes in the environment might trigger larger, abrupt, and irreversible changes and lead to cascading effects. Recent IPCC assessments suggest that tipping points can be achieved between 1° and 2° of warming. Therefore, they are likely to arise at current emissions levels if they have not already occurred. Well-known tipping points concern the Greenland and the West Antarctic ice sheets, the Atlantic Meridional Overturning Circulation (AMOC), thawing permafrost, ENSO, and the

[1]Corresponding author: Francesco Giancaterini, Maastricht University, School of Business and Economics, Department of Quantitative Economics, P.O.box 616, 6200 MD, Maastricht, The Netherlands.
Email: f.giancaterini@maastrichtuniversity.nl.

May 14, 2022

Amazon rainforest. Recent evidence suggests that melting ice sheets is accelerating because of warming temperatures, less snowfall, and ocean warming. Some studies suggest that irreversible disintegration of the Greenland ice sheet could occur at global temperature warming between 0.8° and 3.2° above pre-industrial levels (Wunderling et al. (2021)). An unstoppable ice sheet melting in Antarctica would also be triggered by global warming exceeding 2° (DeConto et al. (2021)). Current ice sheets melting also add fresh water to the North Atlantic, weakening the AMOC, one of the main global ocean currents. The AMOC is already in its weakest state in 1,000 years (Caesar et al. (2021)). Its shut down would cause significant cooling along the US east coast and Western Europe, alter rainfall and cause more drying. A 50% weakening of AMOC could be caused by continued global warming by 2100, and a tipping point could be reached between 3° and 5.5° of warming.

Moreover, the Arctic is warming twice as faster as the planet on average, and it has already warmed 2°, causing permafrost thawing, which releases CO2 and methane into the atmosphere. Available estimates point to 1400 billion tons of carbon frozen in the Arctic's permafrost, twice as much carbon already in the atmosphere, and a 2° of global warming could even cause the thawing of 40% of the world's permafrost. The El Niño-Southern Oscillation or ENSO cycle is an oscillating warming and cooling pattern affecting rainfall intensity and tropics' temperatures. It can strongly influence weather in many parts of the globe. El Niño and La Niña are the warm and cool phases of the ENSO cycle, respectively. Oceans warming can trigger a tipping point in the ENSO cycle, increasing its variability and intensity and shifting its teleconnection eastward (Cai et al. (2021)). Extreme rainfalls and droughts in various parts of the world, not only at the Tropic, can then follow from the destabilization of these natural oscillations. Due to human activity and fires, the Amazon rainforest has already lost about 17% of its tree cover, and at the current rate of deforestation the loss could reach 27% by 2030. Lovejoy and Nobre (2018) estimate the dieback of the Amazon Forest at 20%-25%; beyond this deforestation threshold, the rainforest would transform into a savannah, potentially releasing up to 90 gigatons of CO2. Some climate models already indicate that the Amazon will be a net generator of C02 by 2035, setting the dieback threshold at 3° of warming.

Further uncertainty on the compound effect of the above phenomena arises from their potential interaction, even before the 2° warming is achieved, allowing tipping points to occur at lower thresholds. Overall, greenhouse gases generated by human activity over the last two centuries have driven the global trend temperature up. This temperature warming has widely impacted the natural environment and has raised the risk of irreversible changes of state with catastrophic consequences (see also Schellnhuber (2008)) and Solomon et al. (2009)).

In this paper, we establish a linkage between the concept of environmental tipping point and the statistical property of time irreversibility. A stationary process $\{Y_t\}_{t=1}^{T}$ is said to be time-reversible if its statistical properties are independent of the direction of time. In other words, the vectors $(Y_1, Y_2, \ldots, Y_T)$ have the same joint distributions as $(Y_{-T}, Y_{-(T-1)}, \ldots, Y_{-1})$ for every integer

T. This implies that the processes characterized by time reversibility (TR) exhibit a temporal symmetry in the probabilistic structure. In the alternative circumstance, we have time irreversibility when the stochastic process behaves differently according to the direction of time considered. TR has been under investigation in various fields over the years, for instance, in the different branches of physics, where researchers have been investigating whether time has some preferred direction in explaining physical phenomena (see Wald (1980), Levesque and Verlet (1993), Holster (2003)). This appears to be the case once a tipping point is achieved, where the system undergoes an irreversible state change.

This paper aims to investigate whether TR has the potential to offer insight into the process of climate change, with a particular focus on the process of global warming and its implications for the natural environment. Studying TR in the context of global warming in this paper is motivated by the possibility of answering the following questions: are there divergences between the forward-time and backward-time joint probability distributions for the process of global warming? Is the process of global warming symmetric over time? Are these properties similarly present in natural oscillations that temperature warming might have permanently impacted, inducing changes in their frequencies and intensity of occurrence? Irreversibility in this context might carry insights into the occurrence of state changes.

This paper then introduces new strategies to detect whether a stochastic process is time-reversible. There are already several tests for TR in the econometric literature (see Ramsey and Rothman (1996), Hinich and Rothman (1998), Chen et al. (2000), Belaire-Franch and Contreras (2003), Proietti (2020)). The shortcoming of many of these approaches is that they usually impose strong restrictions on the model (for example, Ramsey and Rothman (1996), which requires finite sixth moments), or they are not trivial to apply (for example, Chen et al. (2000)). Our new strategies are based on mixed causal and noncausal models (see Gourieroux and Jasiak (2016)). Unlike causal models, which only take the relationship between present and lagged values into account, mixed casual and noncausal models also compute the relationship between present and future values. This framework leads to nonlinear conditional expectations (e.g., Gourieroux and Jasiak (2022)). The straightforward connection between these models and TR gives rise to our testing strategies.

Furthermore, similarly to Proietti (2020), we can test for TR on nonstationary time series using a novel approach. To do so, we extract the trend component using the Hodrick-Prescott (HP) filter that is triggered by a time-reversible closed-form solution. This implies that the cyclical component, that records the oscillations of the process around its trend is responsible for the eventual time-irreversibility feature of the stochastic process.

The rest of the paper is as follows. Section 2 summarizes the properties of time-reversible processes. The existing methods to detect TR are briefly reviewed. Section 3 introduces our new TR strategies. Namely, we show how our new approaches exploit the properties of mixed causal and noncausal models. We then evaluate their performance through Monte Carlo experiments. Section 4 extends our framework to nonstationary time series. Section 5 is dedicated to empirical investigations on climate variables. Section 6 concludes.

2. Time reversibility

Weiss (1975) shows that if an ARMA model is characterized by a Gaussian error term, then the process is time-reversible. Indeed, Gaussian processes are completely defined by their second-order moments, which have the property of being time symmetrical.

Hallin et al. (1988) consider two-sided linear models of the form:

$$Y_t = \sum_{k=-\infty}^{\infty} \theta_k \epsilon_{t-k}, \tag{1}$$

where the stationary condition $\sum_{k=-\infty}^{\infty} |\theta_k| < \infty$ is satisfied. They claim that if $\{Y_t\}_{t=1}^{T}$ is time-reversible, then either ϵ_t is a Gaussian white noise, or there exists a k and $s \in \{0,1\}$ such that $\theta_{2k+j} = (-1)^s \theta_{2k-j}$. However, ϵ_t has to be a sequence of *i.i.d.* zero-mean random variables with finite moments of all orders. It is an unrealistic assumption for non-Gaussian processes and many time series.

Breidt and Davis (1992) extend Weiss's results to non-Gaussian processes assuming milder conditions than those in Hallin et al. (1988). They take the following $ARMA(p,q)$ process into account:

$$\phi(L)Y_t = \theta(L)\epsilon_t, \tag{2}$$

where L indicates the backshift operator, $\phi(z)$ is characterized by r roots outside and s roots inside the unit circle, and ϵ_t has finite variance. For simplicity, we set the polynomial $\theta(L) = 1$, such that (2) can be rewritten as:

$$\phi^+(L)\phi^-(L)Y_t = \epsilon_t, \tag{3}$$

where $\phi^+(L)$ has r roots outside the unit circle, while $\phi^-(L)$ has s roots inside. It is well known that (3) has a unique stationary solution given by a two-sided moving average representation, as expressed in (1). Breidt and Davis (1992) claim that if $\phi(z)$ and $\phi(z^{-1})$ have different roots, then Y_t is reversible if and only if the error term is Gaussian. In the other case, that is when the two polynomials $\phi(z)$ and $\phi(z^{-1})$ have the same roots, it can be shown that (1) (or equivalently (3)) is time-reversible regardless of the distribution of ϵ_t. Indeed, if $p > 0$ and $\phi(z)$ and $\phi(z^{-1})$ have the same roots, it can then be shown that $1/\phi(z)$ has the Laurent expansion

$$\frac{1}{\phi(z)} = \sum_{-\infty}^{\infty} \theta_j z^j, \tag{4}$$

with $\theta_{-p/2-j} = \theta_{-p/2+j}$, for $j = 0, 1, \ldots$ (see Breidt and Davis (1992)). This implies that the result of Hallin et al. (1988) is a consequence of the conclusion that the two polynomials $\phi(z)$ and $\phi(z^{-1})$ have the same roots. Moreover, unlike Hallin et al. (1988), Breidt and Davis (1992) only assume that the error term must have finite variance.

Ramsey and Rothman (1996) define the stationary stochastic process $\{Y_t\}_{t=1}^T$ is time-reversible only if:

$$\gamma_{i,j} = E[Y_t^i Y_{t-k}^j] - E[Y_t^j Y_{t-k}^i] = 0 \tag{5}$$

for all $i, j, k \in \mathbb{N}^+$. This is a sufficient condition for TR, but not a necessary one since it only considers a proper subset of moments from the joint distributions of $\{Y_t\}$. Since it's impractical to show that (5) holds for any i, j, and k, they adopt a restricted definition of TR by imposing $i + k \leq m$ and $k \leq K$. In particular, they restrict $m = 3$ so that the symmetric-bicovariance function is given by:

$$\gamma_{2,1} = E[Y_t^2 Y_{t-k}] - E[Y_t Y_{t-k}^2] = 0, \tag{6}$$

for all integer values of k. Ramsey and Rothman (1996) claim that $i + j = 3$ is sufficient to provide a useful indication of time irreversibility.

Ramsey and Rothman (1996) also introduced a new procedure to test TR that became a standard approach to investigating business cycle properties such as asymmetry. It is characterized by a TR test statistic distributed as a standard normal distribution:

$$\sqrt{T}\frac{[\widehat{\gamma}_{2,1} - \gamma_{2,1}]}{\sqrt{Var(\widehat{\gamma}_{2,1})}} \xrightarrow{d} N(0,1), \tag{7}$$

with:

$$\widehat{\gamma}_{2,1} = \widehat{B}_{2,1}(k) - \widehat{B}_{1,2}(k),$$

and:

$$\widehat{B}_{2,1} = (T-k)^{-1} \sum_{t=K+1}^{T} Y_t^2 Y_{t-k} \ ; \quad \widehat{B}_{1,2} = (T-k)^{-1} \sum_{t=K+1}^{T} Y_t Y_{t-k}^2,$$

for various integer values of k. Under the null hypothesis, we have a time-reversible process. It is important to underline that the pre-requisite of the test is that the data must possess a finite first sixth moment. If the distribution lacks those first finite sixth moments, the size of the test can be seriously distorted (see Belaire-Franch and Contreras (2003)).

Chen et al. (2000) propose a new class of tests for TR and, unlike the one proposed by Ramsey and Rothman (1996), they do not require any moment restrictions. This class of tests is based on the following result: if $\{Y_t\}_{t=1}^T$ is a time-reversible process, then for every $k = 1, 2, \ldots,$ the distribution of $X_{t,k} = Y_t - Y_{t-k}$ is symmetric about the origin. The drawback of this approach is that it allows us only to test the symmetry of $X_{t,k}$ for each value of k, giving us no chance to jointly test $X_{t,k}$ for a collection of k values.[2] Finally, its

[2] Chen et al. (2000) state that to jointly test $X_{t,k}$ for a collection of k values, a portmanteau test is required.

implementation is not trivial.

Similar reasoning is adopted by Proietti (2020) since also his test is based on the idea that $X_{t,k}$ has to be symmetric for every $k > 0$. However, the main difference between the two approaches is that the test proposed by Proietti (2020) uses a weaker definition of TR as $\{Y_t\}_{t=1}^T$ can also be nonstationary.

3. New strategies to detect time reversibility on stationary time series

This section introduces new strategies to detect the TR of stationary stochastic processes, exploiting the properties of mixed causal and noncausal models. Breidt et al. (1991) introduce mixed causal and noncausal models as expressed in equation (3). They define the polynomial $\phi^-(z)$ as noncausal and $\phi^+(z)$ as a causal polynomial. In this set up, a required condition for identifying the causal from the noncausal component is the non-Gaussianity of the innovation term.

Lanne and Saikkonen (2011), rewriting the noncausal polynomial in (3) as lead polynomial, start with a mixed causal and noncausal model expressed as:

$$\phi(L)\varphi(L^{-1})Y_t = \epsilon_t, \tag{8}$$

where L^{-1} produces lead such that $L^{-1}Y_t = Y_{t+1}$. A mixed causal and noncausal model represented in this way is denoted as MAR(r,s), where $\varphi(L^{-1})$ is the noncausal polynomial of order s and $\phi(L)$ is the causal polynomial of order r. Purely causal and purely noncausal models are obtained setting respectively $\varphi(L^{-1}) = 1$ and $\phi(L) = 1$ (see Gouriéroux et al. (2013), Hencic and Gouriéroux (2015), Hecq et al. (2016), Fries and Zakoian (2019), Hecq and Voisin (2021), Giancaterini and Hecq (2022), and Fries (2021)). In (8), both causal and noncausal polynomials have their roots outside the unit circle, such that:

$$\phi(z) \neq 0 \;\; and \;\; \varphi(z) \neq 0 \;\; for \;\; |z| \leq 1. \tag{9}$$

The tests for TR that we propose have the common feature of extending the results obtained by Breidt and Davis (1992) to the MAR(r,s) representation (8). This is possible if and only if *Condition* 3.1 is true.

Condition 3.1 A stochastic process that can be expressed as a MAR model is time-reversible if and only if $\phi(z)\varphi(z^{-1})$ have the same roots as $\phi(z^{-1})\varphi(z)$. Namely, when:

$$r = s \; and \; \phi_i = \varphi_i, \;\; for \;\; i = 1, \ldots, s.$$

This implies that MARs are time-reversible if and only if the causal polynomial has the same order and the same coefficients as the noncausal polynomial and vice versa. Remember that it is not possible to identify a MAR model under the Gaussianity of the innovation term. Hence, in that case, we have a time-reversible process (see Weiss (1975)).

3.1. Strategy 1 to detect time reversibility

The first strategy aims to evaluate whether a stochastic process meets *Condition* 3.1. In particular, it uses a procedure that is similar to the one used to identify MAR models (see Lanne and Saikkonen (2011) and Hecq et al. (2016)). That is:

1. We estimate a conventional autoregressive process (also called pseudo causal model) by OLS, and the lag order p ($p = r + s$) is selected using information criteria (for instance, AIC or BIC).
2. We test the normality in the residuals of the AR(p). In the event that the null hypothesis of Gaussianity is not rejected, we cannot identify a MAR(r,s) model and, for the reasons mentioned previously, we have a time-reversible process. Moreover, if the null hypothesis of normality is rejected and p is an odd number, the condition $r = s$ can never be satisfied, and the process is time-irreversible. In the alternative case that the null hypothesis of Gaussianity is rejected, but p is an even number, the condition $r = s$ is a possible scenario and we proceed to the next step.
3. We select a model among all MAR(r,s) specifications with $r + s = p$. This is done using a maximum likelihood approach (see Giancaterini and Hecq (2022) and references therein). In the selection procedure, we also include the model given by the restricted likelihood that imposes commonalities in causal and noncausal parameters. In other words, we are also going to include the model with the same restrictions as in *Condition* 3.1. Note that when we compute the information criteria of the model with restricted likelihood, instead of estimating p parameters, we estimate r (or s) of them, implying a smaller penalty term. Finally, we choose the model with the smallest information criteria.

Let us consider a short example to illustrate how the strategy works. We suppose that we estimate a conventional AR model by OLS, and we reject the Gaussian hypothesis of the residuals, for instance, using the Jarque-Bera test. Furthermore, let us assume we find a number of lags (p) equal to 2. In order to analyze whether our process is time-reversible, we are going to compute the log-likelihoods and then the information criteria of the following four models: MAR(2,0), MAR(0,2), MAR(1,1) as well as the MAR(1,1) with the restriction $\phi = \varphi$. If the model with the smallest information criteria is the one with the restriction, it means that we have a time-reversible process. In the alternative case where another model is selected, then we have a time-irreversible process. The positive aspect of this approach is that it allows us to know with a limited number of steps whether the process is time-reversible. The shortcoming is that the strategy is based on information criteria, which have the property of being very sensitive to the sample, and a specification can be favoured for a tiny difference in the value of those information criteria. We also get the common feature that different criteria lead to different conclusions.

3.2. Strategy 2 to detect time reversibility

The second strategy introduced in this paper is more robust with respect to the sample and slight differences in the value of information criteria when models are compared. On the other hand, more steps are required to identify the TR of the process than for the previous approach. It is based on the following steps: steps 1 and 2 are identical to what we had described in 3.1;

3. we select a model among all MAR(r,s) specifications with $r+s=p$, choosing the one with the largest likelihood (since we are considering models with the same number of parameters).
4. In the event that the selected model is the one with $r=s$, in our previous example, a MAR(1,1), we compute a likelihood ratio test, taking into account the same restrictions as in *Condition* 3.1. If we do not reject the null hypothesis of the test, we have TR. In the opposite case, when the null hypothesis is rejected, we have a time-irreversible process.

3.3. Simulation study

Let us investigate the performance of the two strategies. In particular, we run Monte Carlo simulations with $N = 1000$ replications and four different sample sizes: 100, 200, 500, and 1000 observations (T). The data generating process is a MAR(1,1), that is $(1-\phi L)(1-\varphi L^{-1})Y_t = \epsilon_t$, and different combinations of causal and noncausal coefficients are considered:

- $\phi_0 = 0.8$, $\varphi_0 = 0.8$; time-reversible process;
- $\phi_0 = 0.8$, $\varphi_0 = 0.5$; time-irreversible process;
- $\phi_0 = 0.8$, $\varphi_0 = 0.1$; time-irreversible process.

In all these cases, we assume that the error term is distributed as a Student's-t with degrees of freedom (ν) equal to 3 and a scale parameter (σ) equal to 5. The assumption that the error term is distributed according to a Student's-t is not a particularly strong hypothesis. It is a symmetric distribution that summarizes the features of other (non-Gaussian) fat-tailed and symmetric distributions well. We also include in our Monte Carlo study the results obtained by Ramsey and Rotham's test, setting $k = 2$.

Table 1 shows the frequencies with which the two new strategies and the test proposed by Ramsey and Rotham detect the processes under investigation as time-irreversible; $p = 2$ is assumed to be known, and r and s are estimated. In particular, the columns Strategy 1 and Strategy 2 indicate the percentage of times the stochastic processes are identified as time-irreversible when the strategies introduced in Sections 3.1 and 3.2 are implemented. The last column, *RR* (1996), indicates how often we reject the null hypothesis of TR when the methodology proposed by Ramsey and Rothman (1996) is used. The information criteria used for Strategy 1 is the Bayesian Information Criteria (BIC). The results exhibit that Strategy 1 is the methodology that detects TR with greater precision but is "undersized" for large T. This observation is because the penalty terms can differ from a very small number in a large sample. On the other hand, Strategy 2 looks consistent and is the approach that performs better when the processes under investigation are time-irreversible (frequencies are not size-adjusted, though, which makes the results of Strategies 1 and 2 not easy to compare). The test proposed by Ramsey and Rothman (1996) clearly shows some size distortion problems. This is not an unexpected result since, as previously stated, the test can show a size seriously distorted if the distribution lacks a finite sixth moment. The Student's-t distribution has a finite sixth moment for $\nu > 6$. As a consequence, also the power of the test performs poorly for RR (1996).

MAR(1,1); $\phi_0 = 0.8,\ \varphi_0 = 0.8,\ \nu_0 = 3$			
	Strategy 1	Strategy 2	RR (1996)
T=100	7.9%	18.9%	5.3%
T=200	3.5%	8.5%	7.2%
T=500	1.3%	5.5%	7.2%
T=1000	1.3%	5.6%	9 %
MAR(1,1); $\phi_0 = 0.8,\ \varphi_0 = 0.5,\ \nu_0 = 3$			
	Strategy 1	Strategy 2	RR (1996)
T=100	50%	62.6%	15%
T=200	76.5%	85%	25.2%
T=500	98.4%	99.4%	37.4%
T=1000	100%	100%	58.1 %
MAR(1,1); $\phi_0 = 0.8,\ \varphi_0 = 0.1,\ \nu_0 = 3$			
	Strategy 1	Strategy 2	RR (1996)
T=100	87.7%	5.1%	40.3%
T=200	98.8%	99.1%	54.2%
T=500	100%	100%	68.8%
T=1000	100%	100%	81%

Table 1: *Frequencies with which time irreversibility is detected; MAR(1,1) orders not known.*

However, as Table 2 shows, we obtain different results if we assume that both r and s are known. In this case, we directly compare the information criteria of the restricted and unrestricted MAR(1, 1) for Strategy 1 and, for Strategy 2, we directly compute the likelihood ratio test. The ability of the two new strategies to detect TR further increases for small sample sizes ($T = 100$ and $T = 200$). The results related to the test introduced by Ramsey and Rotham (RR (1996)) are invariant since we applied the same methodology used for Table 1.

MAR(1,1); $\phi_0 = 0.8,\ \varphi_0 = 0.8,\ \nu_0 = 3$			
	Strategy 1	Strategy 2	RR (1996)
T=100	4.3%	6.2%	5.3%
T=200	3%	6.3%	7.2%
T=500	1.3%	5.6%	7.2%
T=1000	1.3%	5.9%	9 %
MAR(1,1); $\phi_0 = 0.8,\ \varphi_0 = 0.5,\ \nu_0 = 3$			
	Strategy 1	Strategy 2	RR (1996)
T=100	47.3%	52.3%	85%
T=200	75.8%	83.4%	74.8%
T=500	98.4%	99.4%	62.6%
T=1000	100%	100%	41.9 %
MAR(1,1); $\phi_0 = 0.8,\ \varphi_0 = 0.1,\ \nu_0 = 3$			
	Strategy 1	Strategy 2	RR (1996)
T=100	84.1%	87%	40.3%
T=200	98.6%	99.4%	54.2%
T=500	100%	100%	68.8%
T=1000	100%	100%	81%

Table 2: *Frequencies with which time irreversibility is detected; MAR(1,1) orders known.*

4. Testing for time reversibility on nonstationary processes

The goal of this section is to detect TR in nonstationary processes $\{Y_t\}_{t=1}^T$ that can be expressed as:

$$Y_t = f_t^Y + cc_t^Y, \tag{10}$$

where f^Y is a generic trend function, and cc^Y is a stationary process that captures the cyclical fluctuations of Y around f^Y. We show that whenever the trend component is computed using the HP filter, then f^Y can be expressed as a time-reversible process. As a consequence, the eventual time irreversibility of process Y would be captured by its cyclical component cc^Y. In other words, whenever f^Y is estimated by using the HP filter, model (10) is time-irreversible (or reversible) if and only if its cyclical component is irreversible (or reversible).

The HP filter estimates the trend component through the following minimization problem (see Hecq and Voisin (2021)):

$$\min_{\{f_t^Y\}_{t=1}^T} \quad \Big(\textstyle\sum_{t=1}^T y_t^2 + \lambda \sum_{t=1}^T \big[(f_t - f_{t-1}) - (f_{t-1} - f_{t-2})\big]^2\Big). \tag{11}$$

According to De Jong and Sakarya (2016), the optimization problem (11) has the following closed-form solution:

$$f_t^Y = \Big(\lambda L^{-2} - 4\lambda L^{-1} + (1+6\lambda) - 4\lambda L + \lambda^2\Big)^{-1} Y_t, \tag{12}$$

for $t = 3, \ldots, T-2$. The λ parameter penalizes the filtered trend's variability; therefore, the higher its value, the smoother the trend component:

$$\lambda = \Big(\frac{number\ of\ observations\ per\ year}{4}\Big)^i,$$

with either $i = 2$ (see Backus and Kehoe (1992)) or $i = 4$ (Ravn and Uhlig (2002)). It can be shown that (12) can be rewritten as:

$$f_t^Y = \Big[\Big(1 - \psi_1(\lambda)L - \psi_2(\lambda)L^2\Big)\Big(1 - \psi_1(\lambda)L^{-1} - \psi_2(\lambda)L^{-2}\Big) + \\ -\Big(\psi_1^2(\lambda) + \psi_2^2(\lambda) + 6\psi_2(\lambda)\Big)\Big]^{-1} Y_t, \tag{13}$$

where $\psi_1(\lambda) = \frac{4\lambda}{\lambda+1}$, and $\psi_2(\lambda) = -\lambda$. For instance, when annual data are considered, it is commonly accepted to adopt $\lambda = 6.25$, implying

$$f_t^Y = \left[\Big(1 - \frac{100}{29}L + 6.25L^2\Big)\Big(1 - \frac{100}{29}L^{-1} + 6.25L^{-2}\Big) - 13.456\right]^{-1} Y_t.$$

The results underline that the filter of the trend component is given by a time-reversible MAR(2,2) polynomial minus a constant value. Since the latter doesn't affect the symmetry over time of our process, and our goal is to investigate the time reversibility of f^Y, we do not consider the constant term in our investigation. As a consequence, we can approximate f^Y as follows:

$$f_t^Y \approx \left[\Big(1 - \frac{100}{29}L + 6.25L^2\Big)\Big(1 - \frac{100}{29}L^{-1} + 6.25L^{-2}\Big)\right]^{-1} Y_t. \tag{14}$$

Using the Laurent expansion as in (4), we have:

$$f_t^Y \approx \sum_{j=-\infty}^{+\infty} \delta_j Y_{t-j}, \tag{15}$$

where because the identity of the lead and lag polynomials, δ is symmetric over time. Hence, even if f^Y is a nonstationary process, we can apply a weaker definition of TR and define it as time-reversible. This implies that the eventual time irreversibility (or reversibility) lies with the cyclical component of Y.

5. Is climate change time-reversible?

We analyze nine different annual climate time series: global land and ocean temperature anomalies (GLO), global land temperature anomalies (GL), global ocean temperature anomalies (GO), solar activity (SA), emissions of greenhouses gas (GHG), emissions of nitrous oxide ($N2O$), Southern Oscillation Index (SOI), North Atlantic Oscillation Index (NAO), and Pacific Decadal Oscillation Index (PDO).[3] GLO, GL, and GO temperature anomalies are employed to measure global warming. They provide the difference between the

[3] GLO, GL, and GO are obtained from https://www.ncdc.noaa.gov/cag/global/time-series. SOI and NAO are obtained from https://www.cpc.ncep.noaa.gov/data/indices/soi and https://www.cpc.ncep.noaa.gov/products/precip/CWlink/pna/norm.nao.monthly.b5001.current.ascii.table, respectively. PDO is obtained from https://www.ncdc.noaa.gov/teleconnections/pdo/. For GHG and SA, the source is Hansen et al. (2017). For $N2O$, we use the historical reconstruction computed in Meinshausen et al. (2017) (data available at https://www.climatecollege.unimelb.edu.au/cmip).

current temperature from a standard benchmark value. Positive temperature anomalies show that the observed temperature is warmer than the benchmark value. Negative temperature anomalies show that the observed temperature is colder than the benchmark value. SOI is one of the most important atmospheric indices for determining the strength of *El Niño* and *La Niña* events and their possible effects on weather conditions in the tropics and various other geographical areas. *El Niño events* are characterized by sustained warming of the central and eastern tropical Pacific, whereas *La Niña* events are characterized by sustained cooling of the same areas. These changes in the Pacific Ocean and its overlying atmosphere occur in a cycle known as the *El Niño–Southern Oscillation* ($ENSO$). High values of SOI indicate *La Niña* events, whereas negative values indicate *El Niño* events. The NAO determine the westerly winds' speed and direction across the North Atlantic and the winter sea surface temperature. When the NAO index is far above average, there is a greater likelihood that seasonal temperatures in northern Europe, northern Asia, and South-East North America will be higher than usual. In contrast, seasonal temperatures in North Africa, North-East Canada, and southern Greenland will be lower than usual. The opposite is true when NAO is far below average. Finally, PDO is a climatic cycle that describes anomalies in sea surface temperature in the Northeast Pacific Ocean. The PDO has the power to influence weather patterns all over North America.

Figure 1 presents the annual data: GLO, GL, GO, SA, GHG, and $N2O$ range from 1881 to 2014, SOI and NAO from 1951 to 2021, and PDO from 1854 to 2021.

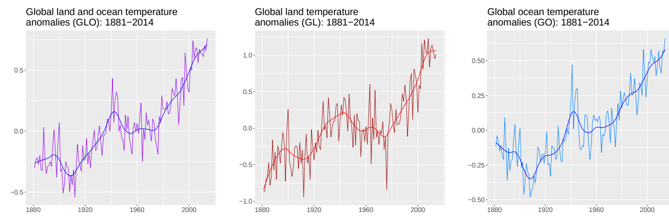

(a) *Annual data for global land and ocean temperature anomalies.*

(b) *Annual data for global land temperature anomalies.*

(c) *Annual data for global ocean temperature anomalies*

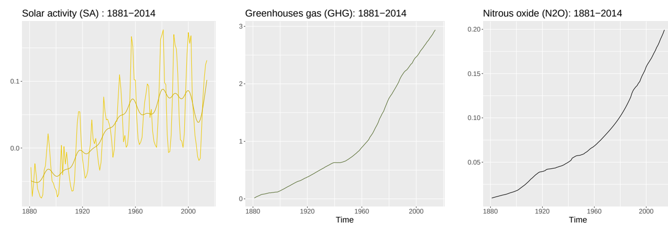

(d) *Annual data for solar activity*

(e) *Annual data for greenhouses gas*

(f) *Annual data for nitrous oxide*

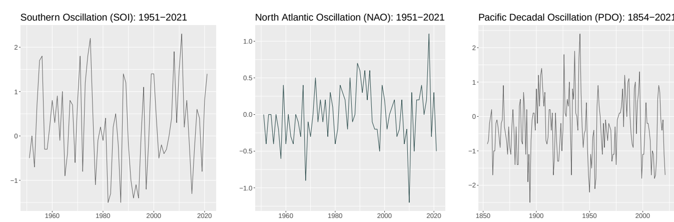

(g) *Annual data for Southern Oscillation index.*

(h) *Annual data for North Atlantic Oscillation index.*

(i) *Annual data for Pacific Decadal Oscillation index.*

Figure 1: Climate time series.

Unlike the natural oscillation indices, GLO, GL, GO, SA, GHG, and $N2O$ are characterized by a positive trend. Hence, according to the strategy introduced in Section 4, their eventual time-reversibility (or irreversibility) lies with their cyclical component. For this reason, we can remove their trend and extract their cyclical fluctuations by using the HP filter. Figure 2 displays the detrended time series.

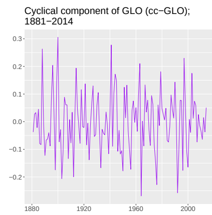

(a) *Annual data for cyclical component of global land and ocean temperature anomalies.*

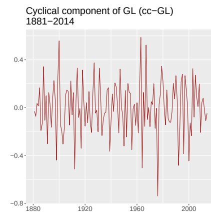

(b) *Annual data for cyclical component of global land temperature anomalies.*

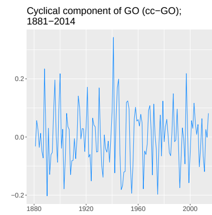

(c) *Annual data for cyclical component of global ocean temperature anomalies.*

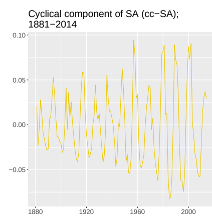

(d) *Annual data for cyclical component of solar activity.*

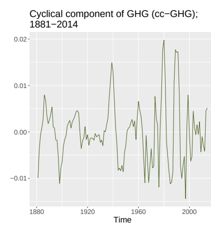

(e) *Annual data for cyclical component of greenhouses gas.*

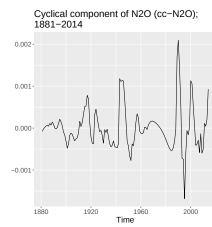

(f) *Annual data for cyclical component of nitrous oxide.*

Figure 2: Cyclical components of the detrended time series.

The goal now is to investigate the time-reversibility of all the variables displayed in Figure 2 and the latter three variables in Figure 1.

As a first step, we estimate autoregressive models (see Sections 3.1 and 3.2) in each time series. The information criteria used to identify the number of lags (p) is the BIC. Next, we test the normality of the residuals of the nine AR(p) models. Since cc^{GLO}, cc^{GL}, cc^{GO}, cc^{SA}, SOI, NAO and PDO do not reject the null hypothesis for normality (significance level 0.05) of the Shapiro-Wilk test (p-values equal to 0.83, 0.59, 0,24, 0.09, 0.16, 0.31, and 0.55 respectively) and the Jarque-Bera test (p-values equal to 0.64, 0.15, 0.25, 0.12, 0.27, 0.31, and 0.55 respectively), we identify them as time-reversible processes. On the other hand, in cc^{GHG} and cc^{N2O}, we reject the null hypothesis of Gaussianity of both the Shapiro-Wilk test (the p-values are close to zero in both cases) and the Jarque-Bera test (the p-values are close to zero in both cases). This implies that we can fit MAR models to our data, identifying cc^{GHG} as MAR(2,0) and cc^{N2O} as MAR(4,0). Since the condition $r = s$ is not met in both cases, we detect these two processes as time-irreversible (Table 3).

	cc^{GHG}: MAR(2,0)	cc^{N2O}: MAR(4,0)
$\hat{\phi}_1$	0.9620	0.9818
	(0.0841)	(0.0722)
$\hat{\phi}_2$	-0.3230	-0.2413
	(0.0822)	(0.0980)
$\hat{\phi}_3$		-0.0016
		(0.1030)
$\hat{\phi}_4$		-0.2028
		(0.0753)
$\hat{\nu}$	19.82	13.03

Table 3: *Estimated coefficients of the cyclical component of GHG and N2O. The figures in parentheses are the standard errors computed by using the Hessian matrix.*

These results let us identify GLO, GL, GO, SA, SOI, NAO, and PDO as time-reversible and GHG, $N2O$ as time-irreversible.

The time irreversibility of cc^{GHG} and cc^{N2O} is a noticeable property of variables that account for the upward trend in global temperatures, i.e., for the global warming phenomenon (IPCC (2014); Morana and Sbrana (2019)). This statistical property should be present in other variables affected by greenhouse gas emissions, as, statistically, a linear combination of time-irreversible and time-reversible variables is also time-irreversible. Finding that the cyclical components of temperatures and natural oscillations such as SOI, NAO, and PDO are not time-irreversible is important. Concerning cyclical temperatures, the finding is consistent with the view that many natural factors (in addition to anthropogenic GHG emissions) can contribute to transitory changes in temperatures. These natural factors include solar and volcanic activity and natural oscillations, such as the $Enso$, the PDO, and the NAO. Apart from the tropics, the strongest $ENSO$ influences are found over North America and Australia, impacting cold conditions over Northern Europe (Chen and Tung (2014), and Bell et al. (2009)).

Coherently, the natural oscillations investigated in the paper do not show the irreversibility property, and their contribution to cyclical temperatures is then dominating the contribution of greenhouse gas emissions. This explains why the irreversibility property, theoretically expected in cyclical temperature, is not detected empirically.

Yet global warming might exert feedback effects on natural oscillations. Tipping points in $AMOC$ and $ENSO$ are, for instance, extreme consequences of warming temperatures in this respect. Oceans warming can trigger a tipping point in the $ENSO$ cycle, increasing its variability and intensity and shifting its teleconnection eastward (Cai et al. (2021); see also Cai et al. (2014), and Cai et al. (2015)). Some empirical evidence of feedback effects of global warming on the natural environment, in terms of higher natural disaster risk induced by Atlantic hurricanes and a destabilizing impact on the $ENSO$ cycle, are reported by Morana and Sbrana (2019). As global warming rises in intensity, its impact on natural oscillation might become detectable through the emergence of the irreversibility feature in these series and, therefore, in cyclical temperatures. Admittedly, while this feature might already be present in the data, we do not empirically detect it. Under a constructive view, our findings then give hope that correction policies might still help avoid the worst consequences of climate change. Yet, they call for action not to miss the opportunity window that appears still available.

6. Conclusions

This paper reviewed and summarized the properties of time-reversible processes. We analyzed the relationship between mixed causal and noncausal models and TR. We exploited their association to create new strategies that help detect TR. In addition to being parsimonious, our simulation studies show that the strategies perform accurately, exhibiting a solid ability to detect TR. Finally, using a weaker definition of TR, we investigate the time reversibility of nonstationary processes. In our empirical investigation, we investigate whether TR appears to be a feature of the process of global warming. In particular, we applied our tests to nine different climate time series: GLO, GL, GO, SA, SOI, NAO, PDO, GHG, and $N2O$. Our new strategies identified the first seven time series as time-reversible and the last two as time-irreversible.

The time irreversibility of GHG emissions is a noticeable property of variables that are well-known causes of global warming. Therefore, we expect to find this property in other variables affected by GHG emissions. In this respect, finding that the cyclical components of temperatures and natural oscillations such as SOI, NAO, and PDO are not time-irreversible is important since global warming might exert feedback effects on the natural environment and raise natural disaster risk. As global warming rises in intensity, its impact on natural oscillation might become detectable through the emergence of the irreversibility feature in these series and, therefore, in cyclical temperatures. Admittedly, while this feature might already be present in the data, the proposed approach cannot detect it.

Further work is needed to allow its implementation within a recursive or moving-window context, which might also provide empirical evidence on the emergence of tipping points, such as those likely to occur once global warming has sufficiently destabilized the natural environment. In this respect, we do not detect such a feature in the sample investigated. Under a constructive view of our findings, while they give hope that correction policies might still be useful to avoid the worst consequences of climate change, they still call for action to not miss the opportunity window that appears still to be available, despite closing quickly.

Acknowledgment

The authors would like to thank the participants of the ECˆ2 2021 (Aarhus) and the CFE 2021 (London) conferences for valuable comments and suggestions.

All remaining errors are ours.

References

Backus, D.K., Kehoe, P.J., 1992. International evidence on the historical properties of business cycles. The American Economic Review , 864–888.

Belaire-Franch, J., Contreras, D., 2003. Tests for time reversibility: a complementarity analysis. Economics Letters 81, 187–195.

Bell, C.J., Gray, L.J., Charlton-Perez, A.J., Joshi, M.M., Scaife, A.A., 2009. Stratospheric communication of el niño teleconnections to european winter. Journal of Climate 22, 4083–4096.

Breidt, F.J., Davis, R.A., 1992. Time-reversibility, identifiability and independence of innovations for stationary time series. Journal of Time Series Analysis 13, 377–390.

Breidt, F.J., Davis, R.A., Lh, K.S., Rosenblatt, M., 1991. Maximum likelihood estimation for noncausal autoregressive processes. Journal of Multivariate Analysis 36, 175–198.

Caesar, L., McCarthy, G., Thornalley, D., Cahill, N., Rahmstorf, S., 2021. Current Atlantic Meridional Overturning Circulation weakest in last millennium. Nature Geoscience 14, 118–120.

Cai, W., Borlace, S., Lengaigne, M., Van Rensch, P., Collins, M., Vecchi, G., Timmermann, A., Santoso, A., McPhaden, M.J., Wu, L., et al., 2014. Increasing frequency of extreme el niño events due to greenhouse warming. Nature climate change 4, 111–116.

Cai, W., Santoso, A., Collins, M., Dewitte, B., Karamperidou, C., Kug, J.S., Lengaigne, M., McPhaden, M.J., Stuecker, M.F., Taschetto, A.S., et al., 2021. Changing El Niño–Southern Oscillation in a warming climate. Nature Reviews Earth & Environment 2, 628–644.

Cai, W., Wang, G., Santoso, A., McPhaden, M.J., Wu, L., Jin, F.F., Timmermann, A., Collins, M., Vecchi, G., Lengaigne, M., et al., 2015. Increased frequency of extreme la niña events under greenhouse warming. Nature Climate Change 5, 132–137.

Chen, X., Tung, K.K., 2014. Varying planetary heat sink led to global-warming slowdown and acceleration. Science 345, 897–903.

Chen, Y.T., Chou, R.Y., Kuan, C.M., 2000. Testing time reversibility without moment restrictions. Journal of Econometrics 95, 199–218.

De Jong, R.M., Sakarya, N., 2016. The econometrics of the hodrick-prescott filter. Review of Economics and Statistics 98, 310–317.

DeConto, R.M., Pollard, D., Alley, R.B., et al., 2021. The Paris Climate Agreement and future sea-level rise from Antarctica. Nature 593, 83–89.

Fries, S., 2021. Conditional moments of noncausal alpha-stable processes and the prediction of bubble crash odds. Journal of Business & Economic Statistics , 1–37.

Fries, S., Zakoian, J.M., 2019. Mixed causal-noncausal ar processes and the modelling of explosive bubbles. Econometric Theory 35, 1234–1270.

Giancaterini, F., Hecq, A., 2022. Inference in mixed causal and noncausal models with generalized student's t-distributions. Econometrics and Statistics, https://doi.org/10.1016/j.ecosta.2021.11.007 .

Gourieroux, C., Jasiak, J., 2016. Filtering, prediction and simulation methods for noncausal processes. Journal of Time Series Analysis 37, 405–430.

Gourieroux, C., Jasiak, J., 2022. Nonlinear forecasts and impulse responses for causal-noncausal (s) var models. Manuscript, University of Toronto .

Gouriéroux, C., Zakoian, J.M., et al., 2013. Explosive bubble modelling by noncausal process. CREST.

Hallin, M., Lefevre, C., Puri, M.L., 1988. On time-reversibility and the uniqueness of moving average representations for non-gaussian stationary time series. Biometrika 75, 170–171.

Hansen, J., Sato, M., Kharecha, P., Von Schuckmann, K., Beerling, D.J., Cao, J., Marcott, S., Masson-Delmotte, V., Prather, M.J., Rohling, E.J., et al., 2017. Young people's burden: requirement of negative co 2 emissions. Earth System Dynamics 8, 577–616.

Hecq, A., Lieb, L., Telg, S., 2016. Identification of mixed causal-noncausal models in finite samples. Annals of Economics and Statistics/Annales d'Économie et de Statistique , 307–331.

Hecq, A., Voisin, E., 2021. Predicting bubble bursts in oil prices using mixed causal-noncausal models. Forthcoming in Advances in Econometrics in honor of Joon Y. Park .

Hencic, A., Gouriéroux, C., 2015. Noncausal autoregressive model in application to bitcoin/usd exchange rates, in: Econometrics of risk. Springer, pp. 17–40.

Hinich, M.J., Rothman, P., 1998. Frequency-domain test of time reversibility. Macroeconomic Dynamics 2, 72–88.

Holster, A., 2003. The criterion for time symmetry of probabilistic theories and the reversibility of quantum mechanics. New Journal of Physics 5, 130.

IPCC, 2014. International panel on climate change fifth assessment report, available at https://www.ipcc.ch/report/ar5/syr/ .

IPCC, 2022. International panel on climate change sixth assessment report, available at https://www.ipcc.ch/report/sixth-assessment-report-cycle/ .

Lanne, M., Saikkonen, P., 2011. Noncausal autoregressions for economic time series. Journal of Time Series Econometrics 3.

Levesque, D., Verlet, L., 1993. Molecular dynamics and time reversibility. Journal of Statistical Physics 72, 519–537.

Lovejoy, T.E., Nobre, C., 2018. Amazon Tipping Point. Science Advances 4, eaat2340.

Meinshausen, M., Vogel, E., Nauels, A., Lorbacher, K., Meinshausen, N., Etheridge, D.M., Fraser, P.J., Montzka, S.A., Rayner, P.J., Trudinger, C.M., et al., 2017. Historical greenhouse gas concentrations for climate modelling (cmip6). Geoscientific Model Development 10, 2057–2116.

Morana, C., Sbrana, G., 2019. Some financial implications of global warming: An empirical assessment. Economic Modelling 81, 274–294.

Proietti, T., 2020. Peaks, gaps, and time reversibility of economic time series. WP Rome .

Ramsey, J.B., Rothman, P., 1996. Time irreversibility and business cycle asymmetry. Journal of Money, Credit and Banking 28, 1–21.

Ravn, M.O., Uhlig, H., 2002. On adjusting the hodrick-prescott filter for the frequency of observations. Review of economics and statistics 84, 371–376.

Schellnhuber, H.J., 2008. Global warming: Stop worrying, start panicking? Proceedings of the National Academy of Sciences 105, 14239–14240.

Solomon, S., Plattner, G.K., Knutti, R., Friedlingstein, P., 2009. Irreversible climate change due to carbon dioxide emissions. Proceedings of the national academy of sciences 106, 1704–1709.

Wald, R.M., 1980. Quantum gravity and time reversibility. Physical Review D 21, 2742.

Weiss, G., 1975. Time-reversibility of linear stochastic processes. Journal of Applied Probability 12, 831–836.

Wunderling, N., Donges, J.F., Kurths, J., Winkelmann, R., 2021. Interacting tipping elements increase risk of climate domino effects under global warming. Earth System Dynamics 12, 601–619.